Lattice Boltzmann method for colloidal dispersions with phase change

B. Piaud[*]

LAboratoire PLAsma et Conversion de l'Energie (LAPLACE),
University of Toulouse, Toulouse, France
E-mail: piaud@laplace.univ-tlse.fr
[*]Corresponding author

M.J. Clifton

Laboratoire de Génie Chimique (LGC),
University of Toulouse, Toulouse, France
E-mail: clifton@chimie.ups-tlse.fr

S. Blanco and R. Fournier

LAboratoire PLAsma et Conversion de l'Energie (LAPLACE),
University of Toulouse, Toulouse, France
E-mail: stb@laplace.univ-tlse.fr
E-mail: rfo@laplace.univ-tlse.fr

Abstract: Colloidal dispersions are known to undergo phase transition in a number of processes. This often gives rise to formation of structures in a flowing medium. In this paper, we present a model for flow of a colloidal dispersion with phase change. Two distribution functions are used. The colloid is described as a non-ideal fluid capable of phase change, but rather than taking the dispersion medium as the second fluid, a better choice is the dispersion (water plus colloid) which can be considered as an incompressible fluid. This choice allows a standard Lattice Boltzmann (LB) model for incompressible fluids to be used in combination with for the 'free-energy' LB model for the colloid. The coupling between the two fluids is the drag force on the colloid and the dependence of the viscosity of the overall fluid on the particle volume fraction. The problems raised by characteristic times and lengths have been treated. The main application considered is the growth dynamics or domain structuration of protein dispersions during dead-end filtration on a membrane surface.

Keywords: colloids; non-ideal fluid; phase transition; Lattice Boltzmann method.

Biographical notes: Benjamin Piaud received his PhD in Physics/Engineering from University of Toulouse in France. He is now a Postdoctoral position at Laboratoire Plasma et Conversion d'Energie (Laboratory on Plasma and Energy Conversion) at University of Toulouse. His research interests include complex fluid flows such as multiphase flows et colloidal dispersions.

Michael J. Clifton is a senior researcher in the Laboratoire de Genie Chimique (Chemical Engineering Laboratory) at the University of Toulouse in France. His general field of interest is membrane filtration, with particular focus on lattice Boltzmann calculations of flow through porous media.

Stéphane Blanco is Maître de Conférence at Laboratoire LAPLACE at the University of Toulouse in France. His fields of interest belong to non-equilibrium statistical thermodynamics and nonlinear physics for application to biology and engineering sciences, with particular focus on self-organisation and morphogenesis.

Richard Fournier is Professeur at Laboratoire LAPLACE at the University of Toulouse in France. His fields of interest belong to non-equilibrium statistical thermodynamics for application to engineering and atmospheric sciences.

1 Introduction

In many industrial processes, colloidal particles are separated from suspensions by means of membrane filtration. The suspending liquid passes through the membrane and the colloidal particles that are held back accumulate in a concentrated, viscous layer at the membrane surface. This phenomenon is known as *concentration polarisation*. If there is flow parallel to the membrane (tangential filtration), this layer quickly reaches a quasi-stationary state, but in the case of dead-end filtration there is only the permeation flow perpendicular to the membrane and the thickness of the layer grows continuously in time. Depending on the permeation rate and on the hydrodynamic conditions, the colloid concentration can become high enough for phase change to take place, leading to formation of a highly viscous gel layer. The presence of this concentrated layer limits the performance of the filtration operation and this is particularly true if a gel layer forms. So it is of practical importance to have a clear understanding of this phenomenon. Rapid phase change in colloids usually corresponds to spinodal decomposition, with domain growth leading to formation of a porous structure. It would be useful to know whether this phenomenon plays a role in membrane filtration and what sort of role. Numerical simulation is particularly attractive in such cases where experimental observation is almost impossible. Macroscopic models do give an overall description of the behaviour of this layer, but to obtain more detailed knowledge of its behaviour it is necessary to apply a different approach such as a Lattice Boltzmann (LB) model. It is known that suspended colloidal particles can be considered as a pseudo-one-component system, showing close analogies with non-ideal vapours (Russel et al., 1989; Likos, 2001), for which LB models already exist. Colloids are somewhat simpler than vapour-liquid systems as the thermal effects they cause are negligible. So to simulate a colloid undergoing flow with phase change it is simply necessary to introduce a model for the behaviour of the suspending liquid (essentially water) whose flow is coupled with the colloid fluid. Such a two-fluid model is not as simple as it appears at first sight: colloidal dispersions undergoing phase change can reach high volume fractions of solid and the density of the carrier fluid is then much reduced. This is why we have chosen to consider the overall fluid (colloid + water) rather than the carrier fluid, as its density is nearly constant and it can be treated by a traditional LB model for incompressible fluids.

In this coupled two-fluid system a great number of phenomena occur and interact: convective and diffusive mass transfer, phase separation with the formation of the interface layer between phases, coupling between the carrier fluid and the colloid particles, viscous flow of the overall fluid with a non-uniform viscosity. Each of these phenomena has characteristic length and time scales. In order to arrive at a satisfactory resolution in space and time, some of these phenomena have to be excluded from the model: this requires careful treatment and so far

the ideal formulation has not been found. The constraints imposed by these different scales are discussed below.

In the present work we have chosen to consider protein solutions as the model colloid medium. Membrane filtration of protein solutions is of great importance in food and pharmaceutical industries and sufficient data are available concerning the osmotic pressure of these solutions. Proteins are macromolecules carrying electric charges and protein solutions are stabilised by the electrostatic repulsions between molecules, while long-range attractive forces are also present and are responsible for phase change. These interactions can be suitably represented by a hard-core double-Yukawa model, for which an analytical equation of state already exists.

2 Model for colloidal dispersion with phase change

The colloidal particles in a suspension can be considered as a fluid with an equation of state relating the osmotic pressure of the suspension $\Pi(\phi)$ to the volume fraction of colloid ϕ. For example, the simplest equation of state for colloidal particles without long-range interaction is the van't Hoff equation $\Pi = nk_bT$ or $\Pi = \phi\frac{k_b}{v_p}T$, with n the concentration of particles, T the temperature, v_p the volume of a particle and k_b Boltzmann's constant. The van't Hoff equation is equivalent to the equation of state of an ideal gas, a fluid whose particles have no long-range interactions. In this work, we consider a suspension of colloidal particles with attractive long-range interactions that allow a phase change to occur. A hard-core double-Yukawa interaction was chosen, as the correponding equation of state can be derived in an analytical form using the mean spherical approximation (Guérin, 2004). Treating the colloids in a suspension as a non-ideal fluid allows us to use a 'free-energy' LB model (Briant et al., 2004; Dupuis and Yeomans, 2005), which is based on the free-energy functional formulation of thermodynamic systems with liquid-vapour interfaces (Rowlinson and Widom, 1982). We must also model the carrier fluid, which is water in most cases. However when the volume fraction of colloid becomes significant, the density of the carrier fluid alone can no longer be considered as constant and this introduces considerable complications. Rather than describe the carrier fluid directly by a second distribution function, we have modelled the overall fluid (water plus colloid) as an incompressible fluid. This choice is reasonable if the colloidal particles have a mass density ($\rho_c = \frac{m_p}{v_p}$, with m_p the mass of one particle) close to that of water ρ_w. This choice precludes any treatment of gravity effects, such as sedimentation, even after coagulation. But in the ultrafiltration process, which is the main application considered here, the effect of sedimentation is negligible. Considering the overall fluid as incompressible allows us to apply a standard LB model for incompressible fluids. The corresponding macroscopic equations of this two-fluid model are:

$$\nabla \cdot \mathbf{u} = 0 \qquad (1)$$

$$\frac{\partial \mathbf{u}}{\partial t} + \mathbf{u} \cdot \nabla \mathbf{u} = -\frac{1}{\rho_0} \nabla p + \nabla \cdot (\nu \nabla \mathbf{u}) \tag{2}$$

for the overall fluid and for the colloidal fluid, we have the compressible Navier-Stokes equation with a pressure tensor derived from the Cahn-Hilliard theory:

$$\partial_t \phi + \partial_\alpha (\phi u_\alpha^c) = 0 \tag{3}$$

$$\partial_t(\phi u_\alpha^c) + \partial_\beta(\phi u_\alpha^c u_\beta^c) = -\frac{1}{\rho_0}\partial_\beta \Pi_{\alpha\beta}$$
$$+ \nu_c \partial_\beta[\phi(\partial_\beta u_\alpha^c + \partial_\alpha u_\beta^c + \delta_{\alpha\beta}\partial_\gamma u_\gamma)] + \phi F_\alpha \tag{4}$$

$\Pi_{\alpha\beta}$ is the osmotic pressure tensor which is derived from the free-energy model for the interface:

$$\Pi_{\alpha\beta} = \left(\Pi_0(\phi) - \frac{\kappa}{2}(\rho_0\partial_\gamma\phi)^2 - \kappa\rho_0^2\phi\partial_{\gamma\gamma}\phi\right)\delta_{\alpha\beta}$$
$$+ \kappa(\rho_0\partial_\alpha\phi)(\rho_0\partial_\beta\phi). \tag{5}$$

Here $\Pi_0(\phi)$ is the equation of state of the colloidal fluid and κ is the parameter related to the surface tension, which is entirely determined by the interaction potential between colloidal particles.

2.1 LB model for overall fluid

The density of the overall fluid is dependent on the volume fraction of colloid $\rho = \phi\rho_c + (1-\phi)\rho_w$. So if $\rho_c \approx \rho_w$, ρ is nearly constant. For our model we assume $\rho = \rho_w = \rho_c = \rho_0$. The overall fluid is described by the $D3Q15$ LB model for incompressible fluids (He and Luo, 1997).

The set of discrete velocity vectors $\mathbf{v_i}$ is $(0,0,0), (\pm c, \pm c, \pm c), (\pm c, 0, 0), (0, \pm c, 0), (0, 0, \pm c)$ with $c = \delta x/\delta t$ (see Fig. 1). The evolution equation for the distribution function of the velocity $\mathbf{v_i}$, $f_i(\mathbf{x}, t)$ is:

$$f_i(\mathbf{x} + \mathbf{v_i}\delta t, t + \delta t) - f_i(\mathbf{x}, t)$$
$$= -\frac{\delta t}{\tau}[f_i(\mathbf{x}, t) - f_i^{eq}(\mathbf{x}, t)] \tag{6}$$

with τ the relaxation time and f_i^{eq} the equilibrium distribution function.

$$f_i^{eq} = w_i\left\{p + p_0\left[3\frac{(\mathbf{v_i} \cdot \mathbf{u})}{c^2} + \frac{9}{2}\frac{(\mathbf{v_i} \cdot \mathbf{u})^2}{c^4} - \frac{3}{2}(\mathbf{u})^2\right]\right\} \tag{7}$$

where w_i are the weight coefficients : $w_i = 2/9$ for $i = 0$, $w_i = 1/9$ for $i = 1, \ldots, 6$ and $w_i = 1/72$ for $i = 7, \ldots, 14$. $p_0 = \rho_0\frac{c^2}{3}$ is a reference pressure. The macroscopic fields which are the pressure p and velocity $\mathbf{u}$ are evaluated by summing the distribution functions f_i.

$$p = \sum_i f_i \tag{8}$$

$$p_0\mathbf{u} = \sum_i \mathbf{v_i} f_i. \tag{9}$$

From the Chapman-Enskog procedure, the macroscopic equations of an incompressible fluid are derived from this

**Figure 1** The D3Q15 set of discrete velocities (taken from Dupuis and Yeomans (2005))
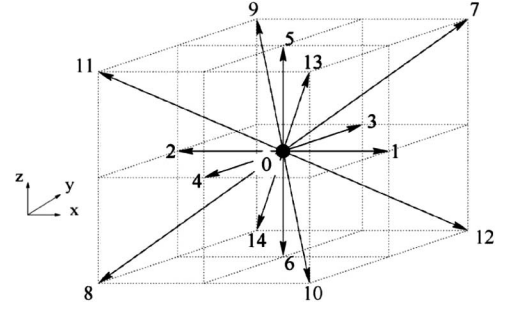
LB model with $\nu = \frac{1}{3}\left(\frac{\tau}{\delta t} - \frac{1}{2}\right)\frac{\delta x^2}{\delta t}$, the kinetic viscosity of the overall fluid. In this work, we take into account the effect of the colloid on the viscosity of the overall fluid. The Eilers-Chong formula (Kissa, 1999) is used for the dependence of viscosity on the volume fraction.

$$\nu(\phi) = \nu_0\left[1 + \frac{1.25\phi}{1 - \phi/\phi_{cp}}\right] \tag{10}$$

with ν_0 the viscosity when $\phi = 0$ and ϕ_{cp} a parameter to fit with experimental values of the viscosity. To introduce this variable viscosity, the relaxation time τ is simply replaced by $\tau(\phi) = 3\frac{\delta t^2}{\delta x^2}\nu(\phi) + \frac{\delta t}{2}$. This method has been numerically tested for Poiseuille flow with a inhomogeneous viscosity in space (cf. Fig. 2). The expression of viscosity is: $\nu(y) = \nu_0 + \alpha y$. The analytical velocity profile for this expression of viscosity is: $u_x(y) = F_x\frac{(L_y - y)\ln(\nu_0) + y\ln(\nu_0 + \alpha L_y) - L_y\ln(\nu_0 + \alpha y)}{2\alpha[\ln(\nu_0) - \ln(\nu_0 + \alpha L_y)]}$, with L_y the width of the channel and F_x the external force which drives the flow.

Figure 2 Velocity profile for a Poiseuille flow with a non-constant viscosity in the channel. The expression of viscosity is: $\nu(y) = \nu_0 + \alpha y$. The solid line represents the analytical profile and circles represent the LB simulations
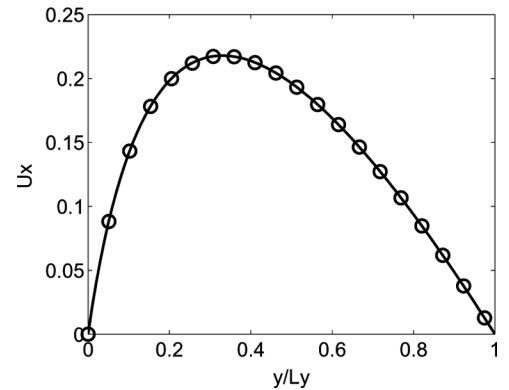
2.2 LB model for the colloidal particles in the suspension

To model the suspension of colloidal particles, which is treated as a non-ideal fluid, we use a $D3Q15$ 'free-energy' LB model (Briant et al., 2004; Dupuis and Yeomans, 2005) with the same set of discrete velocities as for the overall

fluid and with the same time and space discretisation. The evolution equation of the colloid distribution function $g_i(\mathbf{x}, t)$ is:

$$g_i(\mathbf{x} + \mathbf{v_i}\delta t, t + \delta t) - g_i(\mathbf{x}, t)$$
$$= -\frac{\delta t}{\tau_c}[g_i(\mathbf{x}, t) - g_i^{eq}(\mathbf{x}, t)] + 3\phi\, w_i\mathbf{v_i} \cdot \mathbf{F}\,\delta t. \quad (11)$$

Here τ_c is the colloid relaxation time, which physically represents the mean time between collisions for colloidal particles, g_i^{eq} is the equilibrium distribution function (see Appendix A). F_α is the external forcing term which will be presented later. The macroscopic fields which are the volume fraction ϕ and the colloidal fluid velocity $\mathbf{u}^c$ are evaluated by summing the distribution function g_i.

$$\phi = \sum_i g_i \quad (12)$$

$$\phi\mathbf{u}^c = \sum_i \mathbf{v_i}g_i. \quad (13)$$

From the Chapman-Enskog procedure (see Appendix B), the macroscopic equations derived from this LB model are:

$$\partial_t\phi + \partial_\alpha(\phi u_\alpha^c + \frac{\delta t}{2}\phi F_\alpha) = 0 \quad (14)$$

$$\partial_t(\phi u_\alpha^c + \frac{\delta t}{2}\phi F_\alpha) + \partial_\beta(\phi u_\alpha^c u_\beta^c) = -\frac{1}{\rho_0}\partial_\beta\Pi_{\alpha\beta}$$
$$+ \nu_c\partial_\beta[\phi(\partial_\beta u_\alpha^c + \partial_\alpha u_\beta^c + \delta_{\alpha\beta}\partial_\gamma u_\gamma)] + \phi F_\alpha \quad (15)$$

with $\nu_c = \frac{1}{3}(\frac{\tau_c}{\delta t} - \frac{1}{2})\frac{\delta x^2}{\delta t}$ the kinetic viscosity of the colloidal fluid which represents the viscous momentum transfer due to collisons between colloid particles. We note these equations differ from the Equations (3) and (4) by a spurious velocity term $\frac{\delta t}{2}\phi F_\alpha$. In most cases this spurious term can be neglected but as we will see later, for the diffusion regime, this spurious term must be taken into account.

In our two-fluid model, the coupling between the two fluids occurs in two ways. The first is the dependence of the overall-fluid viscosity ν on the volume fraction of the colloid ϕ as seen in Section 2.1. The second coupling is a drag force $\mathbf{F}$ which the carrier fluid exerts on the colloid. The expression for $\mathbf{F}$ is Stokes' law, as corrected by Happel (1958) to account for the effect of the volume fraction on the drag force:

$$\mathbf{F} = H(\phi)\frac{6\pi\mu a}{m_p}(\mathbf{u}^w - \mathbf{u}^c) \quad (16)$$

with μ, the dynamic viscosity of the carrier fluid, $\mathbf{u}^w$ its velocity, a the radius of the colloidal particles and $H(\phi) = \frac{6+4\phi^{5/3}}{6-9\phi^{1/3}+9\phi^{5/3}-6\phi^2}$ the Happel function. But this expression must be re-written as a function of the overall fluid velocity $\mathbf{u}$ because the velocity of the carrier fluid $\mathbf{u}^w$ is not calculated. The relation between these velocities is $\mathbf{u} = \phi\mathbf{u}^c + (1-\phi)\mathbf{u}^w$. So the drag force is:

$$\mathbf{F} = H(\phi)\frac{(\mathbf{u} - \mathbf{u}^c)}{\tau_u(1-\phi)} \quad (17)$$

with $\tau_u = \frac{m_p}{6\pi\mu a}$ a relaxation time, which can be interpreted physically as the characteristic time required for a colloidal particle to reach the same velocity as the carrier fluid.

2.3 Diffusion regime

For colloidal applications, an important simplification can be made in the corresponding macroscopic momentum equation for the colloidal fluid (4). This is the diffusion approximation which consists in keeping only relevant terms in the momentum Equation (4) and considering it as stationary. The advection term and the stress tensor are neglected. So with this approximation and with our expression for the drag force, the corresponding macroscopic equations for the colloidal fluid are:

$$\partial_t\phi + \partial_\alpha\left[\phi u_\alpha^c + \frac{\delta t}{2}\phi H(\phi)\frac{(u_\alpha - u_\alpha^c)}{\tau_u(1-\phi)}\right] = 0 \quad (18)$$

$$\partial_\beta\Pi_{\alpha\beta} = \rho_0\phi H(\phi)\frac{(u_\alpha - u_\alpha^c)}{\tau_u(1-\phi)}. \quad (19)$$

To correctly understand this diffusion approximation, an ideal colloidal fluid can be considered. The pressure tensor is reduced to the van't Hoff equation $\Pi_{\alpha\beta} = \phi\frac{k_b}{v_p}T\delta_{\alpha\beta}$. For a dilute dispersion (i.e., $\phi \ll 1$ and $H(\phi) \rightarrow 1$), Equation (19) corresponds to Fick's first law with an advection term.

$$\phi u_\alpha^c = \phi u_\alpha - D_{th}\partial_\alpha\phi \quad (20)$$

with $D_{th} = \frac{k_b T}{6\pi\mu a}$ the well known diffusion coefficient derived by Einstein (1956). And for the mass-conservation Equation (18), Fick's second law or the diffusion equation is recovered:

$$\partial_t\phi + \partial_\alpha[\phi u_\alpha - D\partial_\alpha\phi] = 0 \quad (21)$$

but with a different diffusion coefficient $D = D_{th}(1 - \frac{\delta t}{2\tau_u})$. This difference appears in the Chapman-Enskog expansion when the forcing term is not neglected in the expression for $g_i^{(1)}$ (see Appendix B).

3 Validation, numerical implementation and results

3.1 Validation of diffusion regime

To test the model and the diffusion regime of our suspension, a series of simulations of a Gaussian peak in ϕ was performed for an ideal dilute colloidal fluid without overall fluid movement (i.e., $\mathbf{u} = 0$). The initial condition is $\phi(x, t=0) = \phi_0 + a\exp[-\frac{(x-x_0)^2}{\sigma^2}]$. The analytical solution for the maximum in the Gaussian peak is $\phi(x = x_0, t) = \phi_0 + \frac{a\sigma}{\sqrt{4Dt+\sigma^2}}$ which allows the diffusion coefficient D to be recovered. This coefficient is also given by Fick's first law $\phi u_\alpha^c = -D_0\partial_\alpha\phi$. Figure 3 shows the diffusion coefficient found by simulations for different values of $\delta t/\tau_u$ (simulations were performed with $\tau_c = \delta t$).

Figure 3 (a) Comparison between the theoretical diffusion coefficient $D_{th} = \frac{k_b T}{6\pi\mu a}$ of an ideal dilute colloidal fluid with D_0 which is obtained from Fick's first law (20) for a series of simulations of diffusion of a Gaussian peak in ϕ with different values of $\delta t/\tau_u$ and (b) circles represent the ratio between the diffusion coefficient D, obtained from Fick's second law (21) and D_{th}. The line represents the theoretical ratio $D/D_{th} = 1 - \frac{\delta t}{2\tau_u}$ predicted by the Chapman-Enskog procedure with the diffusion approximation

(a)

(b)
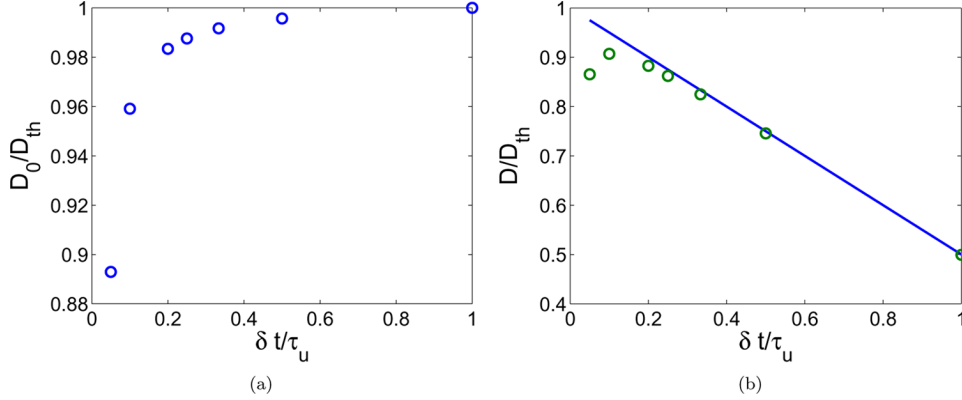
The apparent diffusion coefficient D_0 evaluated by Fick's first law (numerically evaluated by the ratio $D_0 = -\frac{\phi u_\alpha^c}{\partial_\alpha \phi}$), see Figure 3(a) tends towards the theoretical value D_{th} when δt tends towards τ_u. This result means that the diffusion approximation becomes less precise when δt decreases because the stress tensor (which is neglected in the diffusion approximation analysis) becomes more and more important for small values of δt (the expression of colloidal viscosity is $\nu_c = \frac{1}{6}\frac{\delta x^2}{\delta t}$).

The results in Figure 3(b), show the importance of not neglecting the forcing term in the expression for $g^{(1)}$ in the Chapman-Enskog procedure. The δt dependence of the ratio between the two diffusion coefficients, evaluated from Fick's first and second laws, is well reproduced by the simulations.

3.2 Linear stability analysis

To investigate the dynamics of domain growth, during a quench of the colloidal fluid, a linear stability analysis was performed. Rather than doing this analysis on the mesoscopic model, it was performed on the associated macroscopic model with the diffusion approximation (18), (19) in one dimension and without movement of the overall fluid.

$$\frac{\partial \phi}{\partial t} + \frac{\partial}{\partial x}\left[\phi u^c - \frac{\delta t}{2}H(\phi)\frac{u^c}{\tau_u(1-\phi)}\right] = 0 \tag{22}$$
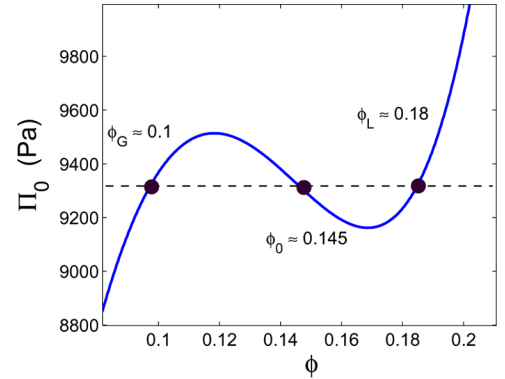
$$\frac{\partial \Pi_0}{\partial x} + \frac{\kappa}{2}\rho_0^2\frac{\partial}{\partial x}\left[\left(\frac{\partial \phi}{\partial x}\right)^2\right] - \kappa\rho_0^2\frac{\partial}{\partial x}\left[\phi\frac{\partial^2\phi}{\partial x^2}\right]$$

$$= -\rho_0 \phi H(\phi)\frac{u^c}{\tau_u(1-\phi)}. \tag{23}$$

The system is perturbed around ϕ_0 and $u_0 = 0$.

$$\phi(x,t) = \phi_0 + \overline{\phi}(x,t) \tag{24}$$

$$u^c(x,t) = \overline{u^c}(x,t) \tag{25}$$

Figure 4 Equation of state derived by Guérin (2004) for a hard-core double-Yukawa interaction. As it follows from the Maxwell's construction, the system separates into two coexisting phase with volume fractions ϕ_G and ϕ_L. ϕ_0 is the unstable equilibrium volume fraction

ϕ_0 is the volume fraction of the unstable equilibrium point as shown in Figure 4. The associated linearised equations for the perturbations are:

$$\frac{\partial \overline{\phi}}{\partial t} + \left[\phi_0 - \frac{\delta t H(\phi_0)}{2\tau_u(1-\phi_0)}\right]\frac{\partial \overline{u^c}}{\partial x} = 0 \tag{26}$$

$$\frac{1}{\rho_0}\Pi_0'(\phi_0)\frac{\partial \overline{\phi}}{\partial x} - \kappa\rho_0\frac{\partial^3\overline{\phi}}{\partial x^3} = -\phi_0 H(\phi_0)\frac{\overline{u^c}}{\tau_u(1-\phi_0)} \tag{27}$$

with $\Pi_0' = \frac{\partial \Pi_0}{\partial \phi}$. In Fourier space we have:

$$\frac{\partial \tilde{\phi}}{\partial t} - ik\left[\phi_0 - \frac{\delta t H(\phi_0)}{2\tau_u(1-\phi_0)}\right]\tilde{u}^c = 0 \tag{28}$$

$$\frac{-ik}{\rho_0}\Pi_0'(\phi_0)\tilde{\phi} - ik^3\kappa\rho_0\tilde{\phi} = -\phi_0 H(\phi_0)\frac{\tilde{u}^c}{\tau_u(1-\phi_0)} \tag{29}$$

where $\tilde{\phi}(k,t)$ and $\tilde{u}(k,t)$ are the Fourier transforms of $\overline{\phi}(x,t)$ and $\overline{u^c}(x,t)$ respectively. So $\tilde{\phi}(k,t)$ and $\tilde{u}(k,t)$ have

Figure 5 Dispersion relation $\omega_+(k)$ for various time steps δt. The results are shown as a function of the ratio $R = \frac{\delta t H(\phi_0)}{2\phi_0 \tau_u (1-\phi_0)}$. The physical result occurs for $\delta t = 0$ (i.e., $R = 0$). The discretisation in time reduces the value of $\omega_+(k)$ but does not change k_m the value of k for which $\omega_+(k)$ is a maximum. The value of k_m is $\sqrt{\frac{-\Pi_0'}{2\rho_0^2 \phi_0 \kappa}}$
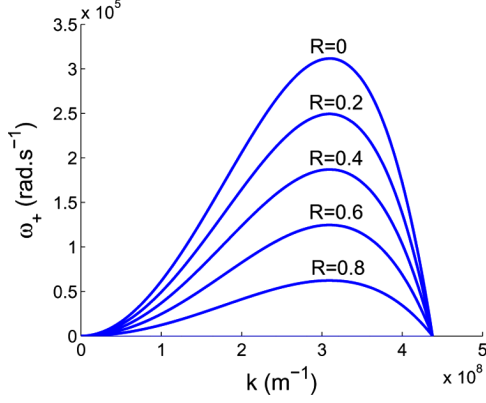
the form of a linear combination of $e^{\omega t}$ with the following dispersion relation (see Fig. 5):

$$\omega(k) = \pm \left[\phi_0 \frac{\tau_u(1-\phi_0)}{H(\phi_0)} - \frac{\delta t}{2} \right] \left[\frac{\Pi_0'}{\rho_0 \phi_0} k^2 + \rho_0 \kappa k^4 \right]. \quad (30)$$

To illustrate the results of the linear stability analysis, a LB simulation of a colloidal fluid quench (see Fig. 6) was performed. The initial condition of the volume fraction field is a random fluctuation around the unstable equilibrium volume fraction ϕ_0. After a few time steps, the initial random fluctuations disappear and only some caracteristic wavelengths persist. In this simulation a domain around 18 nm appears while the linear stability analysis predicts the emergence of wavelengths around $\lambda_m = 2\pi \sqrt{\frac{2\rho_0^2 \phi_0 \kappa}{-\Pi_0'}} \approx 20$ nm. The size of the proteins considered is 3.44 nm, so we can note the colloid aggregates which appear are made up of a small number of particles.

Figure 6 Profile of volume fraction ϕ. The initial condition is a random fluctuation around the unstable equilibrium volume fraction ϕ_0. A characteristic wavelength of about 18 nm appears after a few time steps, which is in agreement with the linear stability analysis
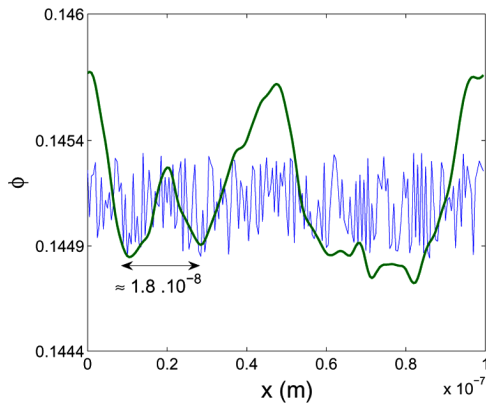
This is because the surface tension of this colloidal system is weak.

3.3 A penalisation method

For the proteins considered, the value of the characteristic time of the drag force is very small, $\tau_u = \frac{m_p}{6\pi\mu a} = 2.63 \; 10^{-12}$ s. As an explicit temporal integration is used, the value of the time step δt must be less than the value of τ_u. This means that, for realistic simulations, the required number time steps is too great. So to perform realistic simulations, we propose a penalisation method which allows a longer time step to be used. For our model this method consists in considering another system $(*)$ for which $\tau_u^* = \varepsilon \tau_u$, $\kappa^* = \kappa/\varepsilon$ and $\Pi_0^* = \Pi_0/\varepsilon$. In according to the Chapman-Enskog procedure, the corresponding macroscopic equations differ from the original system macroscopic Equations (14) and (15) but in the diffusion regime, the same Equations (18) and (19) are recovered. We point out that this penalisation method is applicable because the diffusion regime is relevant for our system. So now, we can solve the $*$ system which can have a greater value of the characteristic time τ_u^* than the original system and so a longer time step can be used. Some LB simulations of a Gaussian peak in ϕ have been made for a wide range of ε values (from 1 to 10^6) and the coefficient diffusion recovered does not depend on the value of ε.

4 Practical implementation

A first set of results has been obtained by simulating dead-end filtration of a solution containing a protein (lysozyme) for which the physico-chemical properties are available, in particular its equation of state (Lin et al., 2002). The ionic strength of the carrier solution was chosen so that the contrast in concentration between the two phases in equilibrium is not too great: 10% and 18%. The size of the domain is $100 \times 40 \times 40$ with $\delta x = 0.5$ nm and $\delta t = 10^{-10}$ s, with periodic boundary conditions on the four (lateral) faces perpendicular to the membrane. On the inlet face (opposite the membrane), the colloid velocity is taken equal to the velocity of the overall fluid and the colloid volume fraction is held constant ($\phi_{in} = 0.145$). A pressure difference Δp is applied between the two sides of the membrane thus leading to a flow velocity of the overall fluid at the membrane, according to the expression: $u_m = L_p(\Delta p - \Pi_m)$, in which L_p represents the hydraulic permeability coefficient of the membrane and Π_m is the osmotic pressure of the colloid at the membrane. In the tests presented, a mean value of Π_m is assumed to apply at the membrane, so u_m is uniform in that plane. If we neglect the effects of spatial variation in the viscosity of the overall fluid (dependent on the colloid volume fraction), and note the periodic boundary conditions on the lateral faces, then the flow of the overall fluid is spatially uniform in the whole domain. The inital field of volume fraction is randomly perturbed around the value ϕ_0 chosen in the unstable zone (cf. Fig. 4): the amplitude of perturbation is 5%.

The calculations show that the phase change is indeed localised in a layer close to the membrane surface, where the initial separation creates 'drops' of condensed and dilute phases. The morphology of these zones is similar to that observed in the quench calculations and the thickness of the layer is also comparable in size to the domain size obtained in quenches. This is also in agreement with the linear stability analysis, even though that analysis did not consider the presence of overall flow. The situation shown in Figure 7 corresponds to a time $5\,\mu$s after the beginning of phase separation: the envelope is an iso-concentration surface used to locate the zone of condensed phase. As for the behavior in time, the concentration close to the membrane is seen to go through a series of oscillations: the condensed layer is unstable as it does not immediately contain enough matter for a complete (and stable) interface to form. This is illustrated by Figure 8 which shows the concentration at the membrane surface as a function of time.

Figure 7 Representation of volume fraction of colloid $\phi\,5\mu$s after the beginning of the phase separation. The domain size is $100 \times 40 \times 40$ with $\delta x = 0.5$ nm and $\delta t = 10^{-10}$ s. The overall flow in the x direction is about 10^{-4} m.s^{-1}, but the colloids are retained by the membrane. The initial condition is a field randomly perturbed around the unstable volume fraction $\phi_0 = 0.145$
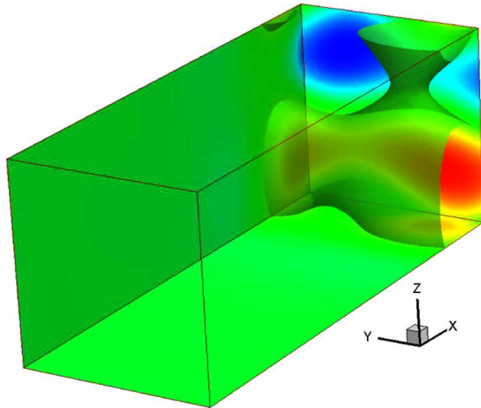

It is known that the permeation rate in ultrafiltration of solutions containing macromolecules (such as proteins) is limited by the presence of these layers of concentrated solution, which often solidify by gellification. The detailed structure of these layers is not observable experimentally, bu it obviously plays a considerable role in determining filtration performance. One question that we wished to answer concerned the possibility that spinodal decomposition could, at least under certain conditions, lead to the formation of a porous structure that could have practical importance. The present results suggest that the phase separation kinetics is indeed fast enough to allow structures to form near the membrane.

To capture the kinetics of phase separation using a LB approach it is necessary to reach high resolutions in both space and time. The thickness of the 'liquid-vapour' interface needs to be resolved and this imposes a quite small value of the space step (0.5 nm): so the overall size of the calculation domain cannot be very great. In the present work the effect of this limitation has been minimised by using periodic coordinates parallel to the membrane surface, but even so the domain size limits the size and the number of 'drops' formed in phase separation.

Figure 8 Representation of the volume fraction at the membrane surface as a function of time. Because of the overall flow, there is an accumulation of colloid at the membrane surface. Oscillations are observed because there is not enough matter for a stable interface to form
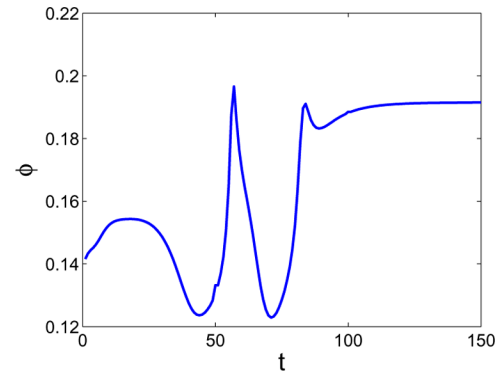
5 Conclusions

In the present tests, the flow of the overall fluid was not calculated. This calculation was made superfluous

- by considering a membrane of uniform permeability
- by neglecting the effects of variable viscosity.

In this way, the effect of the carrier fluid could be replaced by a uniform drag force towards the membrane. However this simplification is not satisfactory as it is known that membranes have both surface roughness and non-uniform permeability on the length scale of the structures produced (Bessières et al., 1996). In principle, the model presented here is capable of representing this sort of phenomenon via the LB solution for the overall fluid. However to implement this methodology in the example shown, the small value of δx and the physical value of the carrier-fluid viscosity impose an extremely small time step $\sim 10^{-14}$ s (i.e., four orders of magnitude smaller than the time step required by the LB treatment of the colloid). The difficulty created by this small time step is particularly severe in view of the number of steps required to go from an initially uniform concentration to a situation where the concentration at the membrane surface reaches an unstable value. In the present tests, the initial concentration was imposed at an already unstable value and the flow rate towards the membrane was fixed at a value ~ 10 times greater than those really met in practice. This problem could be partially solved by using bigger time steps in a first stage where the concentration profile up to the membrane is developing and switching to a more detailed calculation once the condition for phase separation is attained. As for the high flow velocity towards

the membrane, it has been shown in $1D$ calculations that a slower flow towards the membrane lengthens the period of oscillation before the full interface can form. So in a real filtration process, the phase-separation kinetics would be even more favoured than in the present calculations. Obviously a time step of $\sim 10^{-14}$ s is not practical for this type of application. Furthermore, essential physical phenomena at this time scale have already been implicitly neglected, such as for example the relaxation of the electric double layer around the colloid particles (the colloid equation of state assumes an equilibrium state and so neglects this relaxation). So there would be a contradiction in designing a calculation to take account of phenomena on this time scale, particularly as such rapid phenomena are not the ones of interest. Efforts will be required, both on the numerical level and on the level of formulation, to find ways of taking them into account other than by a detailed, explicit numerical representation. A similar problem has already been solved in this work by the penalisation function that was described in Section 3.3.

Acknowledgement

References

Bessières, A., Meireles, M., Coratger, R., Beauvillain, J. and Sanchez, V. (1996) 'Investigations of surface properties of polymeric membranes by near field microscopy', *J. Membrane Sci.*, Vol. 109, p.271–284.

Briant, A.J., Wagner, A.J. and Yeomans, J.M. (2004) 'Lattice Boltzmann simulations of contact line motion. I. Liquid-gas systems', *Phys. Rev. E*, Vol. 69, p.031602.

Dupuis, A. and Yeomans, J.M. (2005) 'Modeling droplets on superhydrophobic surfaces: equilibrium states and transitions', *Langmuir*, Vol. 21, pp.2624–2629.

Einstein, A. (1956) *Investigation on the Theory of the Brownian Movement*, Dover Publications, New York.

Guérin, H. (2004) 'High-temperature expansion of the mean spherical approximation for hard-core two-Yukawa simple and chain fluids', *Fluid Phase Equilibr.*, Vol. 218, pp.47–56.

Happel, J. (1958) 'Viscous flow in multiparticles systems: slow motion of fluids relative to beds of spherical particles', *A.I.Ch.E. Journal*, Vol. 4, p.197.

He, X. and Luo, L-S. (1997) 'Lattice Boltzmann model for the incompressible navier-stokes equation', *J. Stat. Phys.* Vol. 88, pp.927–944.

Kissa, E. (1999) *Dispersions: Characterization, Testing and Measurement*, Marcel Dekker, New York.

Likos, C.N. (2001) 'Effective interactions in soft condensed matter physics', *Phys. Rep.*, Vol. 348, pp.267–439.

Lin, Y.Z., Li, Y.G. and Lu, J.F. (2002) 'Study on osmotic pressures for aqueous lysozyme and alpha-chymotrypsin – Electrolyte solutions with two Yukawa potentials', *J. Colloid Inter. Sci.*, Vol. 251, pp.256–262.

Rowlinson, J.S. and Widom, B. (1982) *Molecular Theory of Capillarity*, Clarendon Press, Oxford.

Russel, W.B., Schowalter, W.R. and Saville, D.A. (1989) *Colloidal Dispersions*, Cambridge University Press, Cambridge.

Appendix A Equilibrium distribution function g_i^{eq}

The equilibrium distribution function has the form of power series in the local velocity (Dupuis and Yeomans, 2005):

$$g_i^{eq} = A_i + B_i v_{i\alpha} u_\alpha^c + C_i u_\alpha^c u_\alpha^c + D_i v_{i\alpha} v_{i\beta} u_\alpha^c u_\beta^c$$
$$+ G_{i\alpha\beta} v_{i\alpha} v_{i\beta} \quad \text{for } i > 0 \tag{31}$$

$$g_0^{eq} = \phi - \sum_{i=1}^{14} g_i^{eq} \tag{32}$$

with

$$A_i = \frac{3w_i}{c^2}(\Pi - \frac{\kappa}{2}(\partial_\alpha \phi)^2 - \kappa \partial_{\alpha\alpha}\phi + \nu_c u_\alpha^c \partial_\alpha \phi) \tag{33}$$

$$B_i = \frac{3w_i\phi}{c^2} \quad C_i = -\frac{3w_i\phi}{2c^2} \quad D_i = \frac{9w_i\phi}{2c^4} \tag{34}$$

$$G_{i\gamma\gamma} = \frac{1}{2c^4}(\kappa(\partial_\gamma \phi)^2 + 2\nu_c u_\gamma^c \partial_\gamma \phi) \quad \text{for } 1 \le i \le 6 \tag{35}$$

$$G_{i\gamma\gamma} = 0 \quad \text{for } i \ge 7 \tag{36}$$

$$G_{i\gamma\delta} = \frac{1}{16c^4}(\kappa(\partial_\gamma \phi)(\partial_\delta \phi) + \nu_c(u_\gamma^c \partial_\delta \phi + u_\delta^c \partial_\gamma \phi)). \tag{37}$$

Appendix B Chapman-Enskog procedure

In this appendix, the Chapman-Enskog procedure is performed on the 'free-energy' LB model with an external forcing term. The LB evolution equation is of the form:

$$g_i(\mathbf{x} + \mathbf{v_i}\delta t, t + \delta t) - g_i(\mathbf{x}, t)$$
$$= -\frac{\delta t}{\tau_c}[g_i(\mathbf{x}, t) - g_i^{eq}(\mathbf{x}, t)] + 3\phi w_i v_{i\alpha} F_\alpha \delta t. \tag{38}$$

This is expanded up to the second order in the time step δt as follows:

$$(\partial_t + v_{i\alpha}\partial_\alpha)g_i + \frac{\delta t}{2}(\partial_t + v_{i\alpha}\partial_\alpha)^2 g_i$$
$$= -\frac{1}{\tau_c}[g_i - g_i^{eq}] + \phi w_i v_{i\alpha} F_\alpha. \tag{39}$$

The zeroth order of Chapman-Enskog procedure consists in approximating g_i by g_i^{eq}. And the second derivatives of g_i^{eq} are negligible compared to the first derivatives.

$$(\partial_t + v_{i\alpha}\partial_\alpha)g_i^{eq} = \phi\, w_i v_{i\alpha} F_\alpha. \tag{40}$$

Then to recover the macroscopic conservation laws, we take the sums of Equation (40), $\sum_i (40)$ and $\sum_i v_{i\alpha} (40)$ and obtain:

$$\partial_t \phi + \partial_\alpha (\phi u_\alpha) = 0 \tag{41}$$

$$\partial_t (\phi u_\alpha) + \partial_\beta P_{\alpha\beta} + \partial_\beta (\phi u_\alpha u_\beta)$$
$$+ \nu_c \partial_\beta (u_\alpha \partial_\beta \phi + u_\beta \partial_\alpha \phi + \delta_{\alpha\beta} u_\gamma \partial_\gamma \phi) = \phi F_\alpha. \tag{42}$$

Here $\nu_c = \frac{1}{3}(\frac{\tau_c}{\delta t} - \frac{1}{2})\frac{\delta x^2}{\delta t}$ is the kinematic viscosity of the colloidal fluid. For the first order of the procedure, g_i is approximated by $g_i^{eq} + g_i^{(1)}$. Using Equation (39), we can obtain an expression for $g_i^{(1)}$ by considering the first derivatives of g_i^{eq} in the left-hand side of the equation.

$$(\partial_t + v_{i\alpha}\partial_\alpha)g_i^{eq} = -\frac{1}{\tau_c}g_i^{(1)} + \phi w_i v_{i\alpha} F_\alpha \tag{43}$$

$$g_i^{(1)} = -\tau_c(\partial_t + v_{i\alpha}\partial_\alpha)g_i^{eq} + \tau_c \phi w_i v_{i\alpha} F_\alpha. \tag{44}$$

So with this expression for g_i, Equation (39) is equivalent to:

$$(\partial_t + v_{i\alpha}\partial_\alpha)g_i^{eq} + \left(1 - \frac{\delta t}{2\tau_c}\right)(\partial_t + v_{i\alpha}\partial_\alpha)g_i^{(1)}$$
$$+ \frac{\delta t}{2}(\partial_t + v_{i\alpha}\partial_\alpha)(\phi w_i v_{i\beta} F_\beta)$$
$$= -\frac{1}{\tau_c}g_i^{(1)} + \phi w_i v_{i\alpha} F_\alpha. \tag{45}$$

So after summing Equation (45) and neglecting terms which are of the order of the Mach number squared, we recover the following macroscopic conservation equation up to the second order in δt.

$$\partial_t \phi + \partial_\alpha \left(\phi u_\alpha + \frac{\delta t}{2}\phi F_\alpha\right) = 0 \tag{46}$$

$$\partial_t \left(\phi u_\alpha + \frac{\delta t}{2}\phi F_\alpha\right) + \partial_\beta(\phi u_\alpha u_\beta) = -\partial_\beta P_{\alpha\beta}$$
$$+ \nu_c \partial_\beta [\phi(\partial_\beta u_\alpha + \partial_\alpha u_\beta + \delta_{\alpha\beta}\partial_\gamma u_\gamma)] + \phi F_\alpha. \tag{47}$$

We note that, because of the forcing term, there is in both equations a spurious flux $u_{spurious} = \frac{\delta t}{2}F_\alpha$, which is negligible in most cases. This spurious flux appears also in the traditional LB model if the forcing term is not neglected in the expression for $g_i^{(1)}$ given by Equation (44).